Draft version May 17, 2021
Typeset using LaTeX **twocolumn** style in AASTeX631

Cosmic Microwave Background map-making solutions with a cooled or perturbative approach

Bai-Qiang Qiang[1] and Kevin M. Huffenberger[1]

[1] Department of Physics, Florida State University, Tallahassee, Florida 32306

ABSTRACT

In the context of the Cosmic Microwave Background, we study the solution to the equation that transforms scanning data into a map. We show that splitting the noise covariance into two parts, as suggested by "messenger" methods for solving linear systems, is particularly effective when there is significant low-frequency noise in the timestream. A conjugate gradient algorithm applied to the modified system converges faster and to a higher fidelity solution than the standard approach, for the same computational cost per iteration. We give an analytical expression for the parameter that controls how gradually the non-uniform noise is switched on during the course of the solution.

Keywords: Computational methods — Cosmic microwave background radiation — Astronomy data reduction

1. INTRODUCTION

In observations of the Cosmic Microwave Background (CMB), map-making is an intermediate step between the collection of raw scanning data and the scientific analyses, such as the estimation of power spectra and cosmological parameters. Next generation CMB observations will generate much more data that today, and so it is worth exploring efficient ways to process the data, even though, on paper, the map-making problem has long been solved.

The time-ordered scanning data is summarized by

$$\mathbf{d} = P\mathbf{m} + \mathbf{n} \tag{1}$$

where $\mathbf{d}$, $\mathbf{m}$, and $\mathbf{n}$ are the vectors of time-ordered data (TOD), the CMB sky-map signal, and measurement noise, and P is the sparse matrix that encodes the telescope's pointing. Of several mapmaking methods (Tegmark 1997a), one of the most common is the method introduced for the Cosmic Background Explorer (COBE, Janssen & Gulkis 1992). This optimal, linear solution is

$$\left(P^\dagger N^{-1} P\right)\hat{\mathbf{m}} = P^\dagger N^{-1}\mathbf{d} \tag{2}$$

where $\hat{\mathbf{m}}$ provides the generalized least squares minimization of the χ^2 statistic

$$\chi^2(\mathbf{m}) \equiv (\mathbf{d} - P\mathbf{m})^\dagger N^{-1}(\mathbf{d} - P\mathbf{m}). \tag{3}$$

Here we assume that the noise has zero mean $\langle \mathbf{n} \rangle = \mathbf{0}$, and noise covariance matrix could be written as $N = \left\langle \mathbf{n}\mathbf{n}^\dagger \right\rangle$. We cast mapmaking as a standard linear regression problem. In case the noise is Gaussian, the COBE solution is also the maximum likelihood solution.

With current computation power, we cannot solve for $\hat{\mathbf{m}}$ by calculating $\left(P^\dagger N^{-1} P\right)^{-1} P^\dagger N^{-1}\mathbf{d}$ directly, since the $(P^\dagger N^{-1} P)$ matrix is too large to invert. The noise covariance matrix N is sparse in frequency domain and the pointing matrix P is sparse in the time-by-pixel domain, and their product is dense. In experiments currently under design, there may be $\sim 10^{16}$ time samples and $\sim 10^9$ pixels, so these matrix inversions are intractable. Therefore we use iterative methods, such as conjugate gradient descent, to avoid the matrix inversions, while executing each matrix multiplication in a basis where the matrix is sparse, using a fast Fourier transform to go between the frequency and time domain.

As an alternative technique, Huffenberger & Næss (2018) showed that the "messenger method" could be adapted to solve the linear mapmaking system, based on the approach from Elsner & Wandelt (2013) to solve the linear Wiener filter. This technique splits the noise covariance into a uniform part and the remainder, and, over the course of the iterative solution, it adjusts the relative weight of those two parts. Starting with the uni-

[1] The source code and other information are available at https://github.com/Bai-Qiang/map_making_perturbative_approach

form covariance, the modified linear system gradually transforms to the final system via a cooling parameter. In numerical experiments, Huffenberger & Næss (2018) found that the large scales of map produced by the cooled messenger method converged significantly faster than for standard methods, and to higher fidelity.

Papež et al. (2018) showed that the splitting of the covariance in the messenger field approach is equivalent to a fixed point iteration scheme, and studied its convergence properties in detail. Furthermore, they showed that the modified system that incorporates the cooling scheme can be solved by other means, including a conjugate gradient technique, which should generally show better convergence properties than the fixed-point scheme. However in numerical tests, Papež et al. (2018) did not find benefits to the cooling modification of the linear system, in contrast to findings of Huffenberger & Næss (2018).

In this paper, we show that the difference arose because the tests in Papež et al. (2018) used much less low-frequency ($1/f$) noise, and show that the cooling technique improves mapmaking performance especially when the low frequency noise is large. This performance boost depends on a proper choice for the pace of cooling. Kodi Ramanah et al. (2017) showed that for Wiener filter the cooling parameter should be chosen as a geometric series. In this work, we give an alternative interpretation of the parameterizing process and show that for map-making the optimal choice (unsurprisingly) is also a geometric series.

KMH: Update this as paper structure changes... In section 2 we briefly introduce messenger field fixed point iteration method and preconditioned version. In section 3 we reinterpret this process and give an analysis on how to determine the parameters. Section 4 gives the noise power spectrum in our simulation, and Section 5 shows results. Finally, Section 6 we discuss this method's pro and con for possible future improvements.

2. METHODS

2.1. *Parameterized Conjugate Gradient Method*

The messenger field approach introduced an extra cooling parameter λ to map-making equation, and solved the linear system with the alternative covariance $N(\lambda) = \lambda\tau I + \bar{N}$. The parameter τ represents the uniform level of (white) noise in the covariance, $\bar{N}$ is the balance of the noise, and the parameterized covariance equals the original covariance when the cooling parameter $\lambda = 1$. In this work we find it more convenient to work with the inverse cooling parameter $\eta = \lambda^{-1}$ and define the covariance as

$$N(\eta) = \tau I + \eta\bar{N} \tag{4}$$

which leads to the same system of mapmaking equations. (This is because $N(\eta) = \lambda^{-1}N(\lambda)$ and the mapmaking equation is insensitive to to scalar multiple of the covariance since is appears on both sides.) Papež et al. (2018) showed that the conjugate gradient method can be easily applied to parameterized map-making equation is

$$P^\dagger N(\eta)^{-1} P\ \hat{\mathbf{m}} = P^\dagger N(\eta)^{-1}\mathbf{d} \tag{5}$$

For simplicity we fix the preconditioner to $M = P^\dagger P$ for all of calculations.

When $\eta = 0$, the noise covariance matrix $N(0)$ is proportional to identity matrix I, and solution is given by simple binned map $\mathbf{m}_0 = \left(P^\dagger P\right)^{-1} P^\dagger \mathbf{d}$, which can be solved directly. From this starting point, the cooling scheme requires the inverse cooling parameter η increase as $0 = \eta_0 \leq \eta_1 \leq \cdots \leq \eta_n = 1$, at which point we are looking at the original system.

Since the non-white part of N is the difficult portion, we could think of the η parameter as turning on slowly, each step adding a perturbation to the solution achieved at a particular stage, building upon the initial the white noise covariance model.

For some intermediate η_i, we use conjugate gradient method to solve equation $\left(P^\dagger N(\eta_i)^{-1} P\right)\hat{\mathbf{m}}(\eta_i) = P^\dagger N(\eta_i)^{-1}\mathbf{d}$ with simple preconditioner $P^\dagger P$, and using $\hat{\mathbf{m}}(\eta_{i-1})$ as the initial value.

2.2. *Choosing inverse cooling parameters η*

The next question is how we choose these monotonically increasing parameters η. If we choose these parameters inappropriately, it makes the system converge slowly, because waste effort converging on the wrong system. We also want to determine $\eta_1, \cdots, \eta_{n-1}$ before starting conjugate gradient iterations. The time ordered data $\mathbf{d}$ is very large, and we do not want to keep it in the system RAM during calculation. If we determine $\eta_1, \cdots, \eta_{n-1}$ before the iterations, then we can precompute the right-hand side $P^\dagger N(\eta)^{-1}\mathbf{d}$ for each η_i and keep these map-sized objects in RAM, instead of the entire time-ordered data.

In the appendix, we show that a good choice for the η parameters are a geometric series

$$\eta_i = \min\left\{\left(2^i - 1\right)\frac{\tau}{\max(\bar{N}_f)},\ 1\right\} \tag{6}$$

This is the main result. It tells us not only how to choose parameters η_i, but also when we should stop the perturbation, and set $\eta = 1$. For example, if noise covariance matrix N is almost white noise, then $\bar{N} = N - \tau I \approx 0$, and we would have $\frac{\tau}{\max(\bar{N}_f)} \gg 1$. This tell us that we don't need to use parameterized method at all, because $\eta_1 = 1$. Note that the vanilla conjugate gradient method with simple binned map as initial guess corresponds to choosing $\eta_0 = 0$ and $\eta_1 = \eta_2 = \cdots = 1$.

2.3. *Intuitive Interpretation of* η

In this section, let me introduce another way to understand the role of η. Our ultimate goal is to find $\hat{\mathbf{m}}(\eta = 1)$ which minimizes $\chi^2(\mathbf{m}) = (\mathbf{d} - P\mathbf{m})^\dagger N^{-1}(\mathbf{d} - P\mathbf{m})$. Since N is diagonal in frequency space, χ^2 could be written as a sum of all frequency mode $|(\mathbf{d} - P\mathbf{m})_f|^2$ with weight N_f^{-1}, such as $\chi^2(\mathbf{m}) = \sum_f |(\mathbf{d} - P\mathbf{m})_f|^2 N_f^{-1}$. N_f^{-1} is large when there is little noise at that frequency, and vice versa. Which means $\chi^2(\mathbf{m})$ would favor the low noise frequency mode over high noise ones. In other words the optimal map $\hat{\mathbf{m}}$ focusing on minimize the error $\mathbf{r} \equiv \mathbf{d} - P\mathbf{m}$ in the low-noise part.

After introducing η, we minimize $\chi^2(\mathbf{m}, \eta) = (\mathbf{d} - P\mathbf{m})^\dagger N_\eta^{-1}(\mathbf{d} - P\mathbf{m})$. For $\eta = 0$, $N_{\eta=0}^{-1} \propto I$ and the estimated map $\hat{\mathbf{m}}(\eta = 0)$ does not prioritize any frequency mode. As we slowly increase η, we decrease the weight for the frequency modes which have large noise, and focusing minimizing error for low noise part. If we start with $\eta_1 = 1$ directly, which corresponds to the vanilla conjugate gradient method, then the entire conjugate gradient solver will only focusing on minimizing low noise part, such that χ^2 would converge very fast at low noise region, but relative slow on high noise part. However by introducing η parameter, we let the solver first treat every frequency equally. Then as η slowly increases, it gradually shifts focus to low noise part.

If we write the difference between final and initial χ^2 value as $\chi^2(\hat{\mathbf{m}}(1), 1) - \chi^2(\hat{\mathbf{m}}(0), 0) = \int_0^1 \mathrm{d}\eta \, \frac{\mathrm{d}}{\mathrm{d}\eta}\chi^2(\hat{\mathbf{m}}(\eta), \eta)$, and use Eq.(B8). We note that when η is very small, the $\frac{\mathrm{d}}{\mathrm{d}\eta}\chi^2(\hat{\mathbf{m}}(\eta), \eta)$ would have relatively large contribution from medium to large noise region, comparing to large η. So introducing η might improve the convergence of χ^2 at these regions, because the vanilla conjugate gradient method only focuses on the low noise part and it may have difficulty at these regions.

2.4. *Computational Cost*

To properly compare the performance cost of this method with respect to vanilla conjugate gradient method with simple preconditioner, we need to compare their computational cost at each iteration. The right hand side of parameterized map-making equation Eq.(5) could be computed before iterations, so it won't introduce extra computational cost. The most demanding part of conjugate gradient method is calculating $P^\dagger N^{-1} P\hat{\mathbf{m}}$, because it contains a Fourier transform of $P\hat{\mathbf{m}}$ from time domain to frequency domain and an inverse Fourier transform of $N^{-1}P\hat{\mathbf{m}}$ from frequency domain back to time domain, which is order $\mathcal{O}(n \log n)$ with n being the length of time ordered data. If we change N^{-1} to $N(\eta)^{-1}$, it won't add extra cost, since both matrices are diagonal in frequency domain. Therefore the computational cost it the same for one step.

However our previous analysis is based on $\chi^2(\hat{\mathbf{m}}(\eta_i), \eta_i)$ which is evaluated at $\hat{\mathbf{m}}(\eta_i)$ the estimated map at η_i. So We should update η_i to η_{i+1} when $\mathbf{m} \approx \hat{\mathbf{m}}(\eta_i)$. How do we know this condition is satisfied? Since for each new η_i value, we are solving a new set of linear equations $A(\eta_i)\hat{\mathbf{m}} = \mathbf{b}(\eta_i)$ with $A(\eta_i) = P^\dagger N(\eta_i)^{-1} P$ and $\mathbf{b}(\eta_i) = P^\dagger N(\eta_i)^{-1}\mathbf{d}$, and we could stop calculation and moving to next value η_{i+1} when the norm of residual $||\mathbf{r}(\eta_i)|| = ||\mathbf{b}(\eta_i) - A(\eta_i)\mathbf{m}||$ smaller than some small value. Calculate $||\mathbf{r}(\eta_i)||$ is part of conjugate gradient algorithm, so this won't add extra cost compare to vanilla conjugate gradient method. Therefore, overall introducing η won't have extra computational cost.

2.5. *Numerical Simulations*

To compare these algorithms, we need to do some simple simulation of scanning processes, and generate time ordered data from random sky signal. Our sky is a small rectangular area, with two orthogonal directions x and y, both with range from -1° to $+1^\circ$. The signal has first three stokes parameters (I, Q, U).

For the scanning process, our single telescope contains nine detectors, each has different sensitivity to polarization Q and U. It scans the sky with a raster scanning pattern and scanning frequency $f_{\text{scan}} = 0.1$ Hz sampling frequency $f_{\text{sample}} = 100$ Hz. The telescope scans the sky horizontally and then vertically, and then digitizes the position (x, y) into 512×512 pixel. This gives noiseless signal $\mathbf{s}$.

The noise power spectrum is given by

$$P(f) = \sigma^2\left(1 + \frac{f_{\text{knee}}^\alpha + f_{\text{apo}}^\alpha}{f^\alpha + f_{\text{apo}}^\alpha}\right) \tag{7}$$

Here we fixed $\sigma^2 = 10\ \mu\text{K}^2$, $\alpha = 2$ and $f_{\text{knee}} = 10$ Hz, and change f_{apo} to compare the performance under different noise models. Note that as $f_{\text{apo}} \to 0$, $P(f) \to \sigma^2\left(1 + (f/f_{\text{knee}})^{-1}\right)$, it becomes a $1/f$ noise model. The noise covariance matrix

$$N_{ff'} = P(f)\frac{\delta_{ff'}}{\Delta_f} \tag{8}$$

is a diagonal matrix in frequency space, where Δ_f is equal to reciprocal of total scanning time T. In our calculations we choose the f_{apo} such that the condition numbers κ are 10^2, 10^6, and 10^12. The corresponding power spectrum are shown in Figure(1).

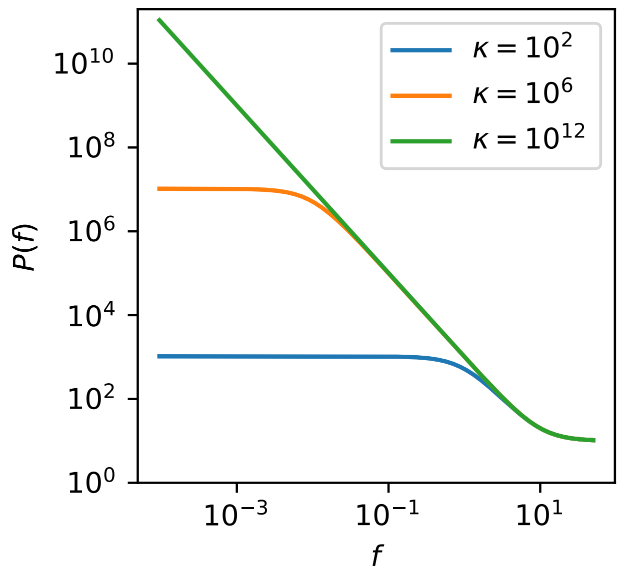

Figure 1. The noise power spectum based on Eq.(7) with $\sigma^2 = 10\ \mu\mathrm{K}^2$, $\alpha = 2$ and $f_{\mathrm{knee}} = 10$ Hz. And fixing the condition number κ of noise covariance matrix Eq.(8) by choosing f_{apo}.

Finally, we get the simulated time ordered data $\mathbf{d} = \mathbf{s} + \mathbf{n}$ by adding up signal and noise.

3. RESULTS

First let's compare the results with vanilla conjugate gradient method with simple preconditioner $P^\dagger P$. The results are showed in Figure.(2) for different kinds of noise power spectra. Here note that χ^2 in all figures are calculated based on Eq.(3) not $\chi^2(\mathbf{m}, \eta)$ in Eq.(A1). The $\chi^2_{\min}$ is calculated from perturbative conjugate gradient method with more intermediate η values, and more iterations after $\eta = 1$.

As we can see in the left graph in Figure(2), when the condition number of noise covariance matrix $\kappa(N)$ is small, the performance between different these two methods are small. The vanilla conjugate gradient method converge faster, because its perturbation parameter goes to 1 at the first iteration, however for the perturbation method its η value will slowly reach 1 in about ten iterations.

Notice that as we increase $\kappa(N)$, or equivalently decrease f_{apo}, the perturbation parameter η starts showing its benefits, as showed in the second and third graph in Figure(2). It outperforms the vanilla conjugate gradient method when $f_{\mathrm{apo}} \approx 0$ and the noise power spectrum becomes the $1/f$ noise model, which usually is the intrinsic noise of instruments (Tegmark (1997b)).

Now let us compare the performance difference between choosing η parameters based on Eq.(A7) and manually fixing number of η parameters n_η manually. We manually choose the η_i values using function `numpy.logspace(start=`$\ln(\eta_1)$`, stop=0, num=`n_η`, base=`e`)`. The results are showed in Figure(3).

When $\kappa(N)$ is small, and Eq.(A7) tells us that only a few η parameters are good enough, see the orange line in the first Figure(3), where we have ~ 10 η levels. If unfortunately we choose n_η being large value, like 15 or 30, then it will ends up converge slowly, because it needs at least 15 or 30 iterations to reach $\eta = 1$, at least one iteration per η level.

On the other hand if $\kappa(N)$ is very large and the power spectrum is $1/f$ noise, we need more η parameters. If n_η is too small, for example $n_\eta = 5$ the green line in last Figure(3), it may be better than the vanilla conjugate gradient method, but it is still far from optimal.

4. FUTURE PROSPECTS AND CONCLUSION

As you may have noticed in the second and third Figure(3), the perturbation parameter based on Eq.(A7) is more than needed, especially for $1/f$ noise case. For the case $\kappa = 10^{12}$, we notice that based on Eq.(A7) it gives us $n_\eta \approx 40$, however from χ^2 result in the last Figure(3) $n_\eta \approx 30$ or even $n_\eta \approx 15$ is good enough. Also, for the nearly-white-noise case, we could certainly choose $n_\eta = 1$ such that $\eta_1 = 1$ which corresponds to vanilla conjugate gradient method, based on χ^2 result in first Figure(3). However Eq.(A7) gives us $n_\eta \approx 6$, even though it does not make the final χ^2 result much different at the end.

Is it possible to further improve the analysis, such that it produces smaller n_η? Let's examine how we get η_i series. Remember that we determine $\delta\eta$ value based on the upper bound of $-\delta\chi^2(\hat{\mathbf{m}}(\eta), \eta)/\chi^2(\hat{\mathbf{m}}(\eta), \eta)$, in Eq.(A3). For $\eta \neq 0$, the upper bound is

$$\delta\eta \frac{\hat{\mathbf{r}}_\eta^\dagger N(\eta)^{-1} \bar{N} N(\eta)^{-1} \hat{\mathbf{r}}_\eta}{\hat{\mathbf{r}}_\eta^\dagger N(\eta)^{-1} \hat{\mathbf{r}}_\eta} \leq \frac{\delta\eta}{\eta + \frac{\tau}{\max(N_f) - \tau}} \tag{9}$$

with $\mathbf{r}_\eta = \left[1 - P\left(P^\dagger N(\eta)^{-1} P\right)^{-1} P^\dagger N(\eta)^{-1}\right]\mathbf{d} \equiv \mathcal{P}_\eta \mathbf{d}$. To get the upper bound we treated $\mathbf{d} - P\hat{\mathbf{m}}(\eta)$ as an arbitrary vector in frequency domain, since we don't know how to calculate $\mathcal{P}_\eta$ for $\eta \neq 0$, and it's hard to analyze the projection matrix $\mathcal{P}_\eta$ in frequency space, as it contains $\left(P^\dagger N(\eta)^{-1} P\right)^{-1}$. Note that we have to determine all of η value before calculation, because we don't want to keep the time ordered data in system RAM, so we need to somehow analytically analyze $\mathcal{P}_\eta$, and its behavior in frequency space. Unless $\mathbf{r}_\eta$ almost only has large noise modes, $\left|\frac{\mathrm{d}}{\mathrm{d}\eta}\chi^2(\hat{\mathbf{m}}(\eta), \eta)/\chi^2(\hat{\mathbf{m}}(\eta), \eta)\right|$ won't get close to the upper bound $1/\left(\eta + \frac{\tau}{\max(N_f) - \tau}\right)$. Based

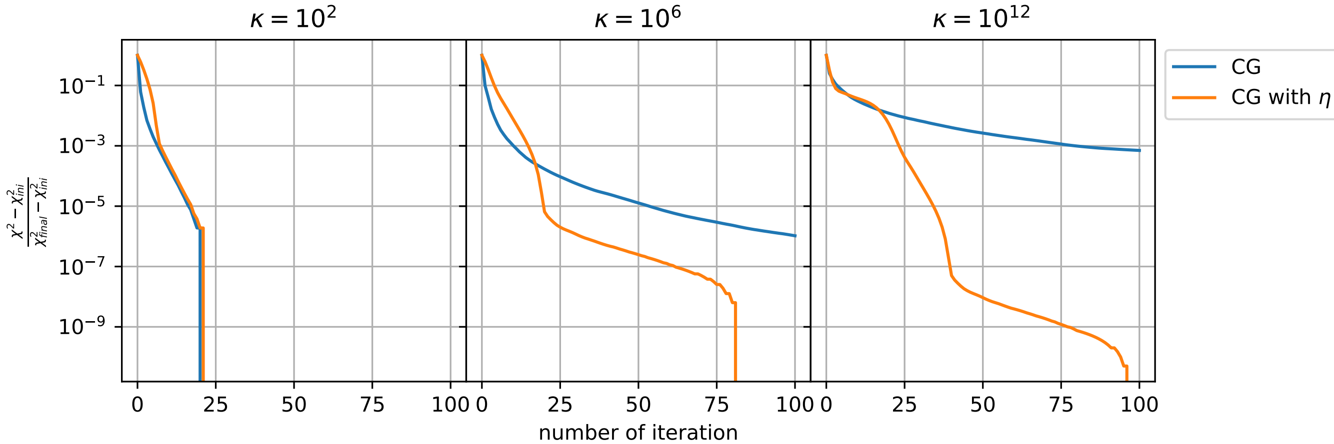

Figure 2. These three figures show the $\frac{\chi^2(\mathbf{m})-\chi^2_{\rm ini}}{\chi^2_{\rm min}-\chi^2_{\rm ini}}$ changes for each iteration under different noise covariance matrix with condition number being 10^2, 10^6, and 10^{12}.

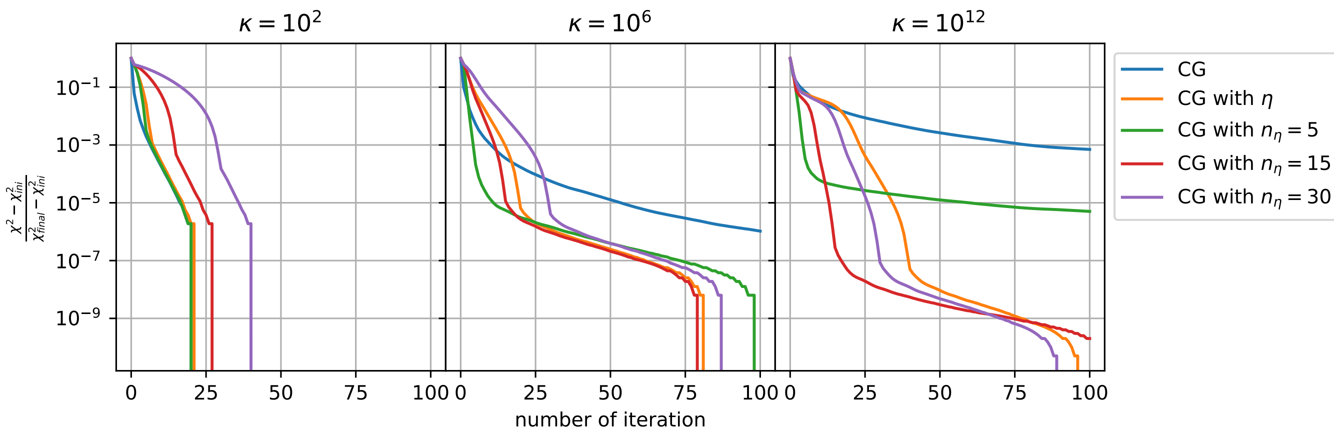

Figure 3. The blue line and the orange line are the same as Figure.(2). For three extra lines, we fix the number of η parameter n_η manully. Instead of using Eq.(A7), we use `numpy.logspace(start=`$\ln(\eta_1)$`, stop=0, num=`n_η`, base=`e`)`. to get all η parameters.

on the analysis in Section(2.3), for small η the estimated map $\hat{\mathbf{m}}(\eta)$ does not only focusing on minimizing error $\mathbf{r}_\eta$ at low noise region. So we would expect that there would be a fair amount of low noise modes contribution in $\mathbf{r}_\eta$ especially for the first few η values. Which means if we could somehow know the frequency distribution of $\mathbf{r}_\eta$, we could tighten the boundary of $\left|\frac{\mathrm{d}}{\mathrm{d}\eta}\chi^2(\hat{\mathbf{m}}(\eta),\eta)/\chi^2(\hat{\mathbf{m}}(\eta),\eta)\right|$, and get larger $\delta\eta$ value. This should make η goes to 1 faster, and yields the fewer η parameters we need.

Also notice that the η values determined from Eq.(A7) are not dependent on any scanning information, it only depends on noise power spectrum $P(f)$, or noise covariance matrix N. In Appendix C we would show two examples with same parameters as in Figure(3) except scanning frequency $f_{\rm scan}$.It turns out the η values should somehow depends on scanning scheme. Again that's because when we determine the upper boundwe treated $\mathbf{r}_\eta$ as an arbitrary vector, such that we lose all information related to scanning scheme in the pointing matrix P.

Even though the perturbation parameter η get from Eq.(A7) are not the most optimal, it still performs much better than traditional conjugate gradient method under $1/f$ noise scenario without adding extra computational cost. The only extra free parameter added is to determine whether the error at current step $\mathbf{r}(\eta_i) = ||\mathbf{b}(\eta_i) - A(\eta_i)\mathbf{m}||$ is small enough such that we advance to next value η_{i+1}.

Also this analysis of η value also explains why cooling parameters $\lambda = 1/\eta$ in messenger field are chosen to be geometric series or `logspace` used in Huffenberger & Næss (2018).

All of the calculation are using simple preconditioner $P^\dagger P$, but the entire analysis is independent of preconditioner. Using better preconditioners, it would also have improvements.

BQ and KH are supported by NSF award 1815887.

APPENDIX

A. THE SEQUENCE OF INVERSE COOLING PARAMETERS

First let us try to find out our starting point η_1. What would be good value for η_1?

Here to simplify notation, I will use N_η to denote $N(\eta)$. The parameterized estimated map $\hat{\mathbf{m}}(\eta) = \left(P^\dagger N_\eta^{-1} P\right)^{-1} P^\dagger N_\eta^{-1}\mathbf{d}$ minimizes the parameterized

$$\chi^2(\mathbf{m},\eta) = (\mathbf{d} - P\mathbf{m})^\dagger N_\eta^{-1}(\mathbf{d} - P\mathbf{m}). \tag{A1}$$

For some specific η value, the minimum χ^2 value is given by

$$\chi^2(\hat{\mathbf{m}}(\eta),\eta) = \big(\mathbf{d} - P\hat{\mathbf{m}}(\eta)\big)^\dagger N_\eta^{-1}\big(\mathbf{d} - P\hat{\mathbf{m}}(\eta)\big) \tag{A2}$$

To further simplify the analysis, let's assume that the noise covariance matrix $N = \left\langle \mathbf{n}\mathbf{n}^\dagger \right\rangle$ is diagonal in the frequency domain.

Let's first consider $\eta_1 = \eta_0 + \delta\eta = \delta\eta$ such that $\eta_1 = \delta\eta$ is very small quantity. Then the relative decrease of $\chi^2(\hat{\mathbf{m}}(0),0)$ from $\eta_0 = 0$ to $\eta_1 = \delta\eta$ is

$$-\frac{\delta\chi^2(\hat{\mathbf{m}}(0),0)}{\chi^2(\hat{\mathbf{m}}(0),0)} = \delta\eta\frac{1}{\tau}\frac{\big(\mathbf{d} - P\hat{\mathbf{m}}(0)\big)^\dagger \bar{N}\big(\mathbf{d} - P\hat{\mathbf{m}}(0)\big)}{\big(\mathbf{d} - P\hat{\mathbf{m}}(0)\big)^\dagger\big(\mathbf{d} - P\hat{\mathbf{m}}(0)\big)} \tag{A3}$$

Here we put a minus sign in front of this expression such that it's non-negative.

Ideally, we want $\delta\chi^2(\hat{\mathbf{m}}(0),0) = \chi^2(\hat{\mathbf{m}}(1),1) - \chi^2(\hat{\mathbf{m}}(0),0)$, such that it would get close to the final χ^2 at next iteration. Here if we assume that initial χ^2 value $\chi^2(\hat{\mathbf{m}}(0),0)$ is much larger than final value $\chi^2(\hat{\mathbf{m}}(1),1)$, then we would expect $\left|\delta\chi^2(\hat{\mathbf{m}}(0),0)/\chi^2(\hat{\mathbf{m}}(0),0)\right| \approx 1^-$, strictly smaller than 1. To make sure it will not start too fast, we could set its upper bound equal to 1, $\delta\eta\max(\bar{N}_f)/\tau = 1$. This gives

$$\eta_1 = \frac{\tau}{\max(\bar{N}_f)} = \frac{\min(N_f)}{\max(N_f) - \min(N_f)} \tag{A4}$$

Here N_f and $\bar{N}_f$ are the eigenvalues of N and $\bar{N}$ under frequency domain. If the condition number of noise covariance matrix $\kappa(N) = \max(N_f)/\min(N_f) \gg 1$, then $\eta_1 \approx \kappa^{-1}(N)$.

What about the other parameters η_m with $m > 1$? We could use a similar analysis, let $\eta_{m+1} = \eta_m + \delta\eta_m$ with a small $\delta\eta_m$, and set the upper bound of relative decrease equal to 1. See Appendix B for detailed derivation. We would get

$$\delta\eta_m = \min\left(\frac{\tau + \eta_m\bar{N}_f}{\bar{N}_f}\right) = \eta_m + \frac{\tau}{\max(\bar{N}_f)}. \tag{A5}$$

Therefore

$$\eta_{m+1} = \eta_m + \delta\eta_m = 2\eta_m + \frac{\tau}{\max(\bar{N}_f)} \tag{A6}$$

As we can see, $\eta_1, \cdots, \eta_n$ increase like a geometric series.

$$\eta_i = \min\left\{1,\ \frac{\tau}{\max(\bar{N}_f)}\left(2^i - 1\right)\right\} \tag{A7}$$

Here we need to truncate the series when $\eta_i > 1$.

B. UPPER BOUND FOR η

We want to find the upper bound for $-\frac{\delta\chi^2(\hat{\mathbf{m}}(\eta_m),\eta_m)}{\chi^2(\hat{\mathbf{m}}(\eta_m),\eta_m)}$ First let's calculate $\frac{\mathrm{d}}{\mathrm{d}\eta}\chi^2(\hat{\mathbf{m}}(\eta),\eta)$

$$\begin{aligned}\frac{\mathrm{d}}{\mathrm{d}\eta}\chi^2(\hat{\mathbf{m}}(\eta),\eta) &= \frac{\partial}{\partial\eta}\chi^2(\hat{\mathbf{m}}(\eta),\eta)\\ &= \frac{\partial}{\partial\eta}\big(\mathbf{d}-P\hat{\mathbf{m}}(\eta)\big)^\dagger N(\eta)^{-1}\big(\mathbf{d}-P\hat{\mathbf{m}}(\eta)\big)\\ &= -(\mathbf{d}-P\hat{\mathbf{m}}(\eta))^\dagger N(\eta)^{-1}\bar{N}N(\eta)^{-1}(\mathbf{d}-P\hat{\mathbf{m}}(\eta))\\ &= -\mathbf{r}^\dagger(\eta)N(\eta)^{-1}\bar{N}N(\eta)^{-1}\mathbf{r}(\eta).\end{aligned} \tag{B8}$$

where the first line comes from, $\chi^2(\hat{\mathbf{m}}(\eta),\eta)$ is minimum χ^2 value for certain η, therefore $\frac{\partial}{\partial\mathbf{m}}\chi^2(\mathbf{m},\eta)\Big|_{\mathbf{m}=\hat{\mathbf{m}}(\eta)}=0$. So the third line we only take partial derivative with respect to $N(\eta)^{-1}$. The last line we define $\mathbf{r}(\eta)=\mathbf{d}-P\hat{\mathbf{m}}(\eta)$.

The upper bound is given by

$$\begin{aligned}-\frac{\delta\chi^2(\hat{\mathbf{m}}(\eta_m),\eta_m)}{\chi^2(\hat{\mathbf{m}}(\eta_m),\eta_m)} &= \delta\eta_m\frac{\mathbf{r}^\dagger N(\eta_m)^{-1}\bar{N}N(\eta_m)^{-1}\mathbf{r}}{\mathbf{r}^\dagger N(\eta_m)^{-1}\mathbf{r}}\\ &\le \delta\eta_m\ \max\left(\frac{\bar{N}_f}{\tau+\eta_m\bar{N}_f}\right)\end{aligned} \tag{B9}$$

For the last line, both matrix $\bar{N}$ and $N(\eta_m)^{-1}$ can be simultaneously diagonalized in frequency space. For each eigenvector $\mathbf{e}_f$, the corresponding eigenvalues of the matrix $N(\eta_m)^{-1}\bar{N}N(\eta_m)^{-1}$ are $\lambda_f=\bar{N}_f(\tau+\eta_m\bar{N}_f)^{-2}$, and the eigenvalues for matrix $N(\eta_m)^{-1}$ are $\gamma_f=(\tau+\eta_m\bar{N}_f)^{-1}$. Their eigenvalues are related by $\lambda_f=\frac{\bar{N}_f}{\tau+\eta_m\bar{N}_f}\gamma_f$. For vector $\mathbf{r}=\sum_f\alpha_f\mathbf{e}_f$, we have $\frac{\mathbf{r}^\dagger N(\eta_m)^{-1}\bar{N}N(\eta_m)^{-1}\mathbf{r}}{\mathbf{r}^\dagger N(\eta_m)^{-1}\mathbf{r}}=\frac{\sum_f\alpha_f^2\lambda_f}{\sum_f\alpha_f^2\gamma_f}=\frac{\sum_f\alpha_f^2\gamma_f\bar{N}_f/(\tau+\eta_m\bar{N}_f)}{\sum_f\alpha_f^2\gamma_f}\le\max\left(\frac{\bar{N}_f}{\tau+\eta_m\bar{N}_f}\right)$.

If we set the upper bound $\delta\eta_m\max\left(\frac{\bar{N}_f}{\tau+\eta_m\bar{N}_f}\right)=1$, [1] and then we get

$$\delta\eta_m=\min\left(\frac{\tau+\eta_m\bar{N}_f}{\bar{N}_f}\right)=\eta_m+\frac{\tau}{\max(\bar{N}_f)}. \tag{B10}$$

C. OTHER CASES

Since the η values determined from Eq.(A7)

$$\eta_i=\min\left\{1,\ \frac{\tau}{\max(\bar{N}_f)}\left(2^i-1\right)\right\} \tag{A7}$$

are not dependent on any scanning information, it only depends on noise power spectrum $P(f)$, or noise covariance matrix N. Figure.(4) and Figure.(5) show two examples with same parameters as in Figure.(3) except scanning frequency f_{scan} (also we need to change f_{apo} to fix condition number), in Figure.(4) it scans very slow and in Figure.(5) it's very fast. In these two cases under $1/f$ noise model, our η values based on Eq.(A7) are better than manually selected values. Based on these two results we know, the η values should somehow depends on scanning scheme.

REFERENCES

Elsner, F., & Wandelt, B. D. 2013, A&A, 549, A111, doi: 10.1051/0004-6361/201220586

Huffenberger, K. M., & Næss, S. K. 2018, The Astrophysical Journal, 852, 92, doi: 10.3847/1538-4357/aa9c7d

[1] Here we also assumed that $\chi^2(\hat{\mathbf{m}}(\eta_m),\eta_m)\gg\chi^2(\hat{\mathbf{m}}(1),1)$, which we expect it to be satisfied for $0\simeq\eta_m\ll 1$. Since final result Eq.(A7) is geometric series, only a few η_m values won't satisfy this condition.

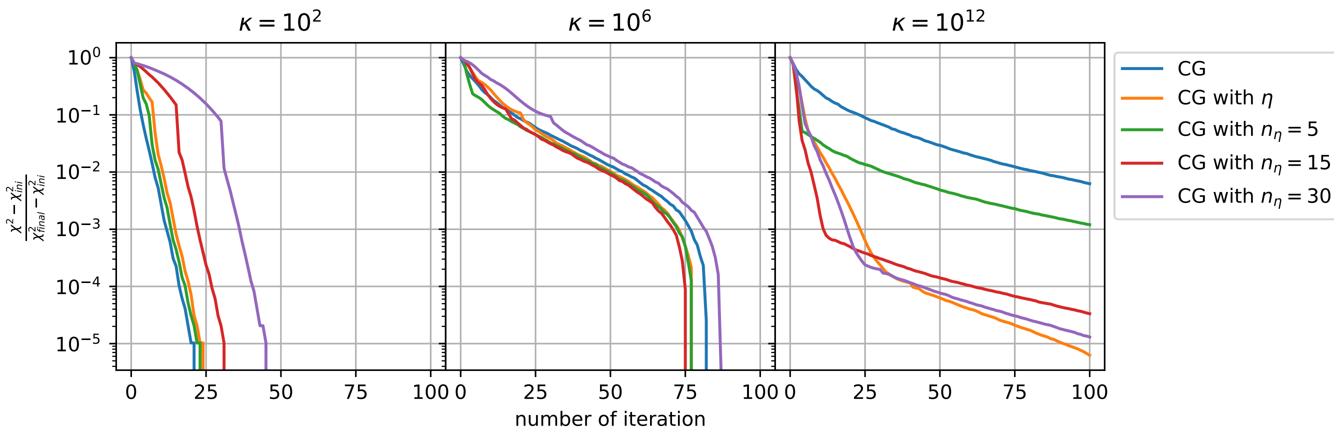

Figure 4. In this case all parameters are the same as Figure.(3) except $f_{\rm scan} = 0.001$, and corresponding $f_{\rm apo}$ to fix the condition number.

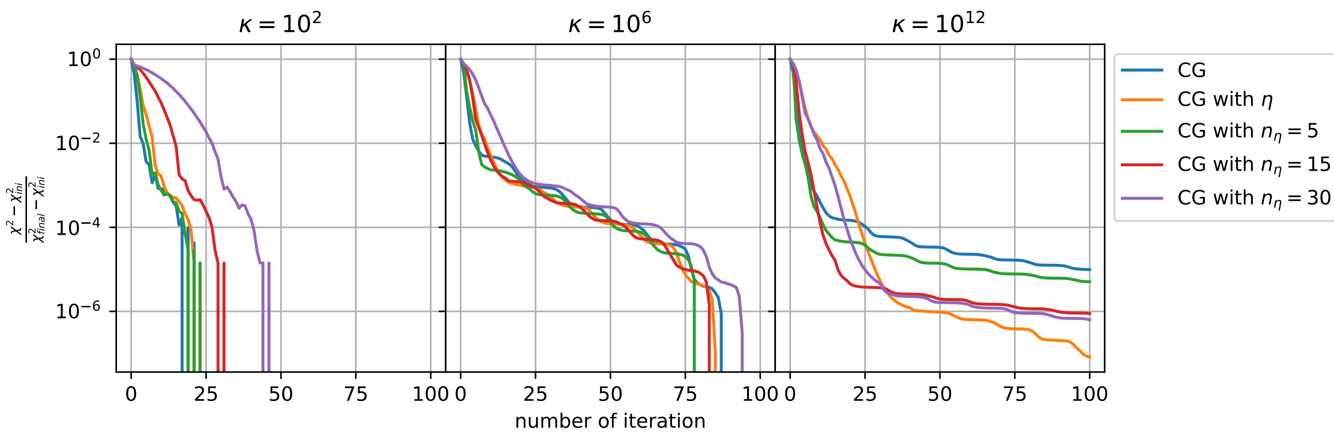

Figure 5. In this case all parameters are the same as Figure.(3) except $f_{\rm scan} = 10$, and corresponding $f_{\rm apo}$ to fix the condition number.

Janssen, M. A., & Gulkis, S. 1992, in NATO Advanced Science Institutes (ASI) Series C, ed. M. Signore & C. Dupraz, Vol. 359 (Springer), 391–408

Kodi Ramanah, D., Lavaux, G., & Wandelt, B. D. 2017, MNRAS, 468, 1782, doi: 10.1093/mnras/stx527

Papež, J., Grigori, L., & Stompor, R. 2018, A&A, 620, A59, doi: 10.1051/0004-6361/201832987

Tegmark, M. 1997a, ApJL, 480, L87, doi: 10.1086/310631

—. 1997b, PhRvD, 56, 4514, doi: 10.1103/PhysRevD.56.4514